

Pleiotropic Effects of *CEP290* (*NPHP6*) Mutations Extend to Meckel Syndrome

Lekbir Baala,* Sophie Audollent,* Jéléna Martinovic, Catherine Ozilou, Marie-Claude Babron, Sivanthiny Sivanandamoorthy, Sophie Saunier, Rémi Salomon, Marie Gonzales, Eleanor Rattenberry, Chantal Esculpavit, Annick Toutain, Claude Moraine, Philippe Parent, Pascale Marcorelles, Marie-Christine Dauge, Joëlle Roume, Martine Le Merrer, Vardiella Meiner, Karen Meir, Françoise Menez, Anne-Marie Beaufrère, Christine Francannet, Julia Tantau, Martine Sinico, Yves Dumez, Fiona MacDonald, Arnold Munnich, Stanislas Lyonnet, Marie-Claire Gubler, Emmanuelle Génin, Colin A. Johnson, Michel Vekemans, Féréchté Encha-Razavi, and Tania Attié-Bitach

Meckel syndrome (MKS) is a rare autosomal recessive lethal condition characterized by central nervous system malformations, polydactyly, multicystic kidney dysplasia, and ductal changes of the liver. Three loci have been mapped (*MKS1*–*MKS3*), and two genes have been identified (*MKS1/FLJ20345* and *MKS3/TMEM67*), whereas the gene at the *MKS2* locus remains unknown. To identify new MKS loci, a genomewide linkage scan was performed using 10-cM-resolution microsatellite markers in eight families. The highest heterogeneity LOD score was obtained for chromosome 12, in an interval containing *CEP290*, a gene recently identified as causative of Joubert syndrome (JS) and isolated Leber congenital amaurosis. In view of our recent findings of allelism, at the *MKS3* locus, between these two disorders, *CEP290* was considered a candidate, and homozygous or compound heterozygous truncating mutations were identified in four families. Sequencing of additional cases identified *CEP290* mutations in two fetuses with MKS and in four families presenting a cerebro-reno-digital syndrome, with a phenotype overlapping MKS and JS, further demonstrating that MKS and JS can be variable expressions of the same ciliopathy. These data identify a fourth locus for MKS (*MKS4*) and the *CEP290* gene as responsible for MKS.

Meckel syndrome (MKS [MIM 249000]) is an autosomal recessive lethal condition characterized by the association of CNS malformations (typically occipital meningoencephalocele), postaxial polydactyly (PD), multicystic kidney dysplasia, and ductal proliferation in the portal area of the liver. In addition, the clinicopathological diversity of MKS phenotypes has led to the distinction of Meckel-like syndrome, or Goldston syndrome groups (MIM 267010). MKS is genetically heterogeneous, and two genes have been identified—*MKS1* on 17q¹ and *TMEM67* (*MKS3*) on 8q,² which encode proteins required for primary cilium formation³—whereas *MKS2* at 11q13 remains unknown.⁴ Each of these three loci accounts for ~10% of cases,⁵ which suggests the existence of further genetic heterogeneity.

To identify new MKS loci, a genomewide scan was performed in eight families unlinked to *MKS1*, *MKS2*, or *MKS3* loci, with use of microsatellite markers spaced 10 cM apart. The highest heterogeneity LOD (HLOD) score was found at marker *D12S326* (HLOD = 2.45; proportion of linked families = 0.6) (fig. 1a and 1b). Five affected siblings from four consanguineous families showed homozygosity for two consecutive microsatellite markers on chromosome 12 (families 1, 2, 11, and 12) (fig. 1c). In family 3, parents were not reported to be related but originated from the same region (Gabes and Mareth) of southern Tunisia. The two affected siblings were therefore analyzed by Affymetrix 10K SNP chips (version 2.1), and only a single common homozygous region was observed, on a 10-Mb interval on chromosome 12q21 (29 consecutive SNPs) (fig. 2a). Hap-

From the INSERM U781 (L.B.; S. Sivanandamoorthy; M.L.M.; A.M.; S.L.; M.V.; F.E.-R.; T.A.-B.) and U574 (S. Saunier; R.S.; M.-C.G.), Université René Descartes (L.B.; C.E.; M.L.M.; A.M.; S.L.; M.V.; F.E.-R.; T.A.-B.), Département de Génétique (S.A.; J.M.; C.O.; A.M.; S.L.; M.V.; F.E.-R.; T.A.-B.), and Service Maternité (Y.D.), Hôpital Necker-Enfants Malades, Service de Génétique et d'Embryologie Médicales, Hôpital Armand Trousseau (M.G.), Service d'Anatomie Pathologique, Hôpital Bichat (M.-C.D.), Service de Biologie du Développement, Hôpital Robert Debré (F.M.), and Service d'Anatomopathologie, Hôpital Saint-Vincent de Paul (J.T.), Assistance Publique-Hôpitaux de Paris, Paris; INSERM U535 and Université Paris Sud, Villejuif, France (M.C.-B.; E.G.); West Midlands Regional Genetics, Birmingham Women's Hospital, Birmingham, United Kingdom (E.R.; F.M.); Service de Génétique, Centre Hospitalo-Universitaire Hôpital Bretonneau, Tours, France (A.T.; C.M.); Département de Pédiatrie et Génétique Médicale et Laboratoire d'Anatomopathologie, Centre Hospitalier Régional Universitaire, Hôpital Morvan, Brest, France (P.P.; P.M.); Génétique Médicale, Centre Hospitalier Intercommunal, Poissy, Saint-Germain-En-Laye, France (J.R.); Department of Human Genetics and Pathology, Hadassah University Hospital, Jerusalem (V.M.; K.M.); Services d'Anatomie Pathologique et Génétique Médicale, Hôpital Hôtel Dieu, Clermont-Ferrand, France (A.M.-B.; C.F.); Service d'Anatomopathologie, Centre Hospitalier Intercommunal de Créteil, Créteil, France (M.S.); and Section of Ophthalmology and Neurosciences, Leeds Institute of Molecular Medicine, St. James's University Hospital, Leeds, United Kingdom (C.A.J.)

Received January 17, 2007; accepted for publication March 30, 2007; electronically published June 4, 2007.

Address for correspondence and reprints: Dr. Tania Attié-Bitach, Département de Génétique et INSERM U-781, Hôpital Necker-Enfants Malades, 149 rue de Sèvres, 75743 Paris Cedex 15, France. E-mail: tania.attie@necker.fr

* These two authors contributed equally to this work.

Am. J. Hum. Genet. 2007;81:170–179. © 2007 by The American Society of Human Genetics. All rights reserved. 0002-9297/2007/8101-0017\$15.00
DOI: 10.1086/519494

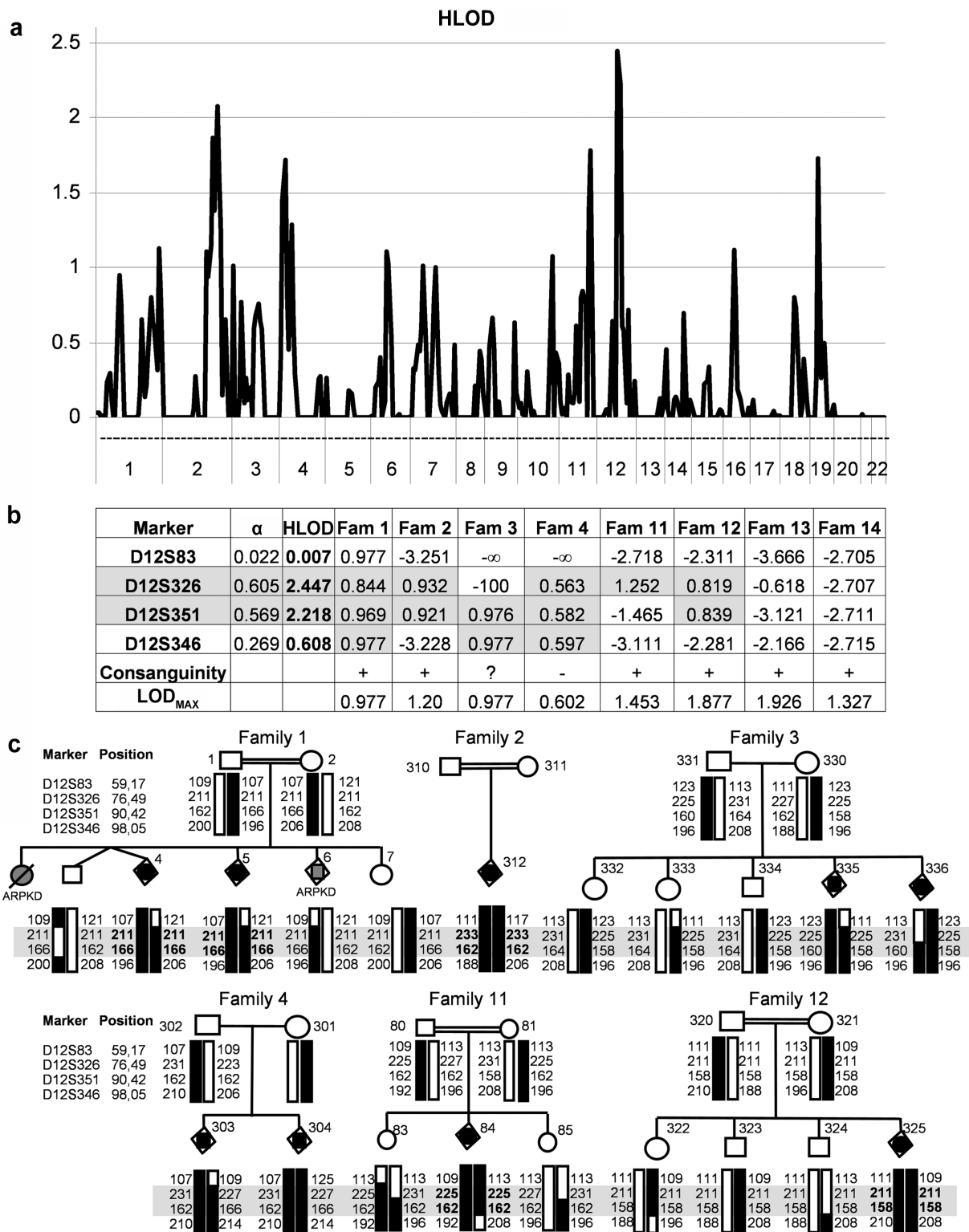


Figure 1. Genomewide scan. *a*, Results of the multipoint linkage analysis with microsatellite markers performed in eight families (Fam), with use of MERLIN software⁶ under the assumption of a fully penetrant recessive model with a disease-allele of frequency of 0.0001 and with allowance for heterogeneity between families. The highest HLOD score (2.45) was found at marker *D12S326*. *b*, Summary of HLOD observed at chromosome 12 in each of the eight families. Six of the eight families show a LOD score at a marker *D12S326*, *D12S351*, or *D12S346* close to its maximal value (LOD_{max}). *c*, Haplotyping at the 12q21 locus in the six families showing potential linkage to chromosome 12. Homozygosity for two consecutive markers—*D12S326* and *D12S351* (boxed)—is observed in five affected siblings of four families (1, 2, 11, and 12). In family 1, the first child and case 6 (gray) are affected with ARPKD.

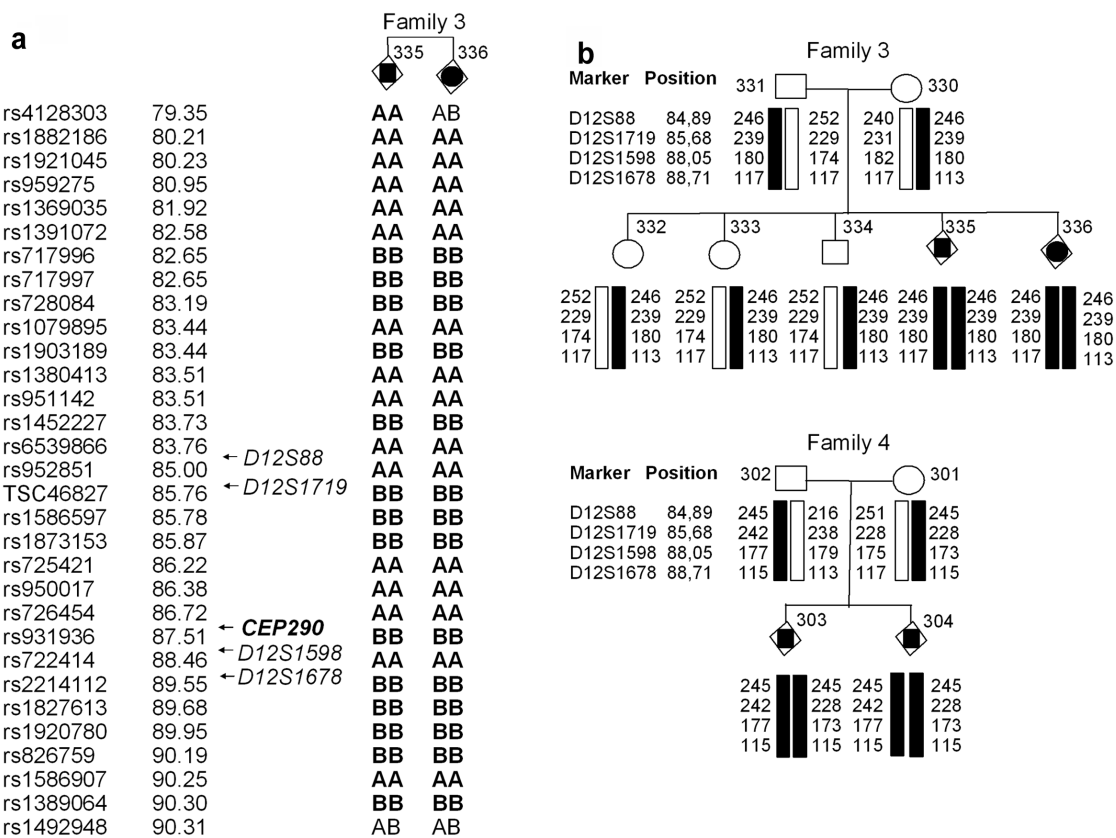


Figure 2. Haplotype analysis of families 3 and 4. *a*, Haplotyping analysis with Affymetrix 10K SNP chips of affected siblings 335 and 336 of family 3, which identified a single homozygous region on chromosome 12¹ between markers *rs1882186* and *rs1389064*. This 10-Mb region includes *CEP290*. *b*, Analysis of four microsatellite markers flanking *CEP290* in family 3, which confirmed homozygosity in only affected siblings 335 and 336 and reduced the telomeric boundary of the interval to position 88.71 (*D12S1678*). In family 4 carrying the same maternally inherited p.Asp128GlufsX34 mutation as family 3, the maternal disease haplotype is different from fetuses 335 and 336 and does not suggest a founder effect for the mutation. Positions of SNP and microsatellite markers are given according to the UCSC Genome Browser database.

lotype analysis with microsatellite markers flanking *CEP290* confirmed homozygosity in fetuses but not in unaffected siblings and reduced the telomeric boundary to position 88.7 Mb (fig. 2*b*). This smallest interval of 8 Mb contained *CEP290*, a gene encoding a centrosomal protein recently identified as the Joubert syndrome (JS [MIM 213300]) gene at the *JBTS5* locus,^{8,9} also found to be frequently mutated in isolated Leber congenital amaurosis (LCA [MIM 204000]).^{10,11} JS is another autosomal recessive ciliopathy, characterized by a combination of neurological signs¹² and a “molar tooth sign” (MTS) on axial images that is associated with cerebellar vermis hypoplasia/dysplasia.¹³ Variable features include retinal dystrophy, renal anomalies, PD, and occipital encephalocele (OE) defining the JS-related disorders or cerebello-oculo-renal syndrome (CORS). Mutations/deletions in three genes have been identified as responsible for JS: *AH11* (*JBTS3*, 6q23.2),¹⁴ *NPHP1* (*JBTS4*, 2q13),¹⁵ and *CEP290* (*JBTS5*, 12q21),^{8,9} whereas two more genes remain unknown: *JBTS1/CORS1* at 9q34.3¹⁶ and *JBTS2/CORS2* at 11p12-11q13.3.^{17,18}

In view of the phenotypic overlap between JS and MKS and our recent finding of allelism at the *MKS3* locus between these two disorders,¹⁹ *CEP290* was considered an excellent candidate gene. Sequencing of the 53 coding exons revealed homozygous truncating mutations in families 1, 2, and 3 and compound heterozygous mutations in family 4, confirming that *CEP290* is the gene for MKS on chromosome 12. Sequencing of 20 additional MKS cases (all negative for mutations in *MKS1* and *TMEM67*) identified two additional MKS-affected families with affected individuals carrying compound heterozygous mutations of *CEP290* (families 5 and 6). Finally, we identified mutations in four families presenting a cerebro-reno-digital syndrome, with a phenotype between that of MKS and JS and thus representing the continuum spectrum between these two disorders (families 7–10). Clinical data are summarized in table 1, and mutations are shown in figure 3.

In families 1–6, when autopsy was performed, MKS was diagnosed for all fetuses on the basis of the association of a brain malformation, MKS cystic kidneys (fig. 4*a–4d*), and

bile-duct proliferation (BDP) of liver (table 1 and fig. 4e–4h). occipital meningocele (OM) was present in at least one sibling in 5 of 6 families, which was associated with a Dandy-Walker malformation (DWM) or vermis agenesis in some cases. In all siblings of family 3 and in subject 4 of family 1, the DWM was the only brain malformation. Detailed neuropathological examination of seven cases assumed to have DWM showed brain-stem disorganization in addition to the severe cerebellar vermis hypoplasia (table 1 and fig. 4i–4k). Transverse sections at the level of the pons showed elongated and thickened peduncles resulting in an inverted molar tooth aspect in four subjects (table 1 and fig. 4k). In subject 3501, the fourth ventricle (V4) distortion/dilatation was more severe, and no MTS was observed (fig. 4j). Among the other signs and with consideration of the affected siblings for whom no DNA was available, PD was present in two of six families (6 of 14 subjects), intrauterine growth retardation (IUGR) affected one subject (subject 4), *situs inversus* and asplenia were present in one fetus (fetus 408), microphthalmia was present in one fetus (fetus 312), and cardiac septal defects were present in two fetuses (fetuses 0114 and 650).

In addition to these six fetuses with MKS, *CEP290* mutations were identified in four families (families 7–10) whose conditions were considered “Meckel-like” because of the absence of at least one characteristic feature required for the diagnosis of MKS. In fetus 385 of family 7, no BDP of liver was observed. In family 8, the molecular screening was performed despite heterozygosity at the *CEP290* locus in fetus 712 from consanguineous Palestinian parents. At histology, the fetus, at 18 wk gestation, presented cystic kidneys with liver ductal plate proliferation characteristic of MKS but with an isolated vermis hypoplasia as brain malformation. In families 9 and 10, which each had two affected siblings, a DWM that was associated with OE was present in one sibling but not the other. At neuropathological examination, however, major abnormalities of the brain stem and the cerebellum were present in all four fetuses, with thickened cerebellar peduncles, severe vermis hypoplasia, and disorganized corticospinal tracts at the pons level (fig. 4p and 4q). Kidneys were macroscopically normal in family 9, with microcystic formations involving mainly the medullary collecting tubes at histology (fetus 381 [fig. 4l]), and were characteristic of MKS in family 10 (fetus 05/158 [fig. 4m]). The liver was either unremarkable (fetus 380) or showed moderate/focal ductal plate anomalies (fetus 381 [fig. 4n] and fetus 05/158 [fig. 4o]). Postaxial PD was present in fetuses 385 and 380, and no other visceral malformation was observed.

The mutations were all nonsense, frameshift, or splice-site mutations, predicting a truncated protein in absence of RNA-mediated decay. Interestingly, the p.Asp128GlufsX34 mutation, homozygous in the patients from Tunisian family 3, was also found but in the heterozygous state in the fetus from family 4, where it was inherited from the mother of French origin. Haplotyping by microsatellite

markers at the *CEP290* locus showed that different alleles (fig. 2b) were associated with this mutation, suggesting a recurrent mutation rather than a founder effect. This mutation was also reported in a patient with LCA.¹¹ Therefore, a mutational hotspot may exist at this position. Another possible mutational hotspot at 3175A or nearby could also be suggested. A deletion (c.3175delA) was identified in Tunisian family 2, whereas an insertion of a single A at the same position was identified in two patients originating from Denmark⁸ and France,¹¹ and a T deletion at the next base (c.3176delT) was found in a Turkish patient with JS.²⁰ The p.Leu1884ThrfsX23 mutation identified in family 6 was reported elsewhere in three families of French origin^{11,21} and one German family.⁸ In addition, the compound heterozygous mutation in family 6 (p.Leu1884-ThrfsX23+p.Phe1950LeufsX15) was also present in a living patient with JS reported by Tory et al.²¹

In MKS, the most common CNS malformations include posterior OE, prosencephalic dysgenesis, and rhombic roof dysgenesis.²² However, other malformations, such as DWM, hydrocephalus, and agenesis of the corpus callosum, are described as occasional features. Diagnosis of DWM is based on vermis hypoplasia/agenesis and cystic dilatation of the V4. Vermis hypoplasia/agenesis and V4 dilatation may also be features of MTS, which is considered characteristic of JS. In fetuses, the distinction between these two malformations is not easy to discern. MTS is characterized by hypoplastic brain stem and dysmorphic V4, flanked laterally with thick cerebellar peduncle. The V4 is usually moderately dilated. The vermis is severely hypoplastic, reduced to a few folia. In all cases reported here, the brain malformation initially reported as DWM consisted, after careful neuropathological examination, of a severe vermis hypoplasia with brain-stem dysplasia. In eight fetuses, the malformation was associated with OE or OM.

Fetal cases with an incomplete phenotype such as isolated vermis hypoplasia (family 7), normal brain with few tubular medullary cysts (family 9), or normal or discrete liver changes (families 6, 9, and 10) are regrouped in a clinically heterogeneous group of disorders referred to as “Meckel-like syndrome.” We recently showed a kidney phenotypic overlap between MKS and Bardet-Biedl syndrome (BBS [MIM 209900]), another recessive disorder ascribed to a ciliary function defect.²³ More recently, we found that MKS-like-affected subjects could carry *TMEM67* gene mutations and that *TMEM67* was also a disease-causing gene for JS.¹⁹ Here, we report 10 cases of *CEP290*-mutated fetuses, with a continuum of clinical 2spectrum from JS to MKS, with either the brain malformation or the kidney or liver anomalies, reinforcing the notion of clinical spectrum and/or overlap among ciliary phenotypes.

Pleiotropic effects of *CEP290* mutations are even more striking, since *CEP290* mutations were recently shown to be a frequent cause of isolated LCA.¹⁰ A genotype-phenotype correlation was suggested, since all LCA-affected patients of the study of den Hollander et al.¹⁰ carried the

Table 1. Clinical Data and Mutations of CEP290-Mutated Fetuses

Family, Subject, and Nucleotide Change(s)	Parental Origin	Exon	Predicted Effect on Protein	Age (gw) ^a	Origin	PD	CKD/MKS ^b	BDP	Cleft Palate	Phenotypic Features									
										CNS Initial Diagnosis ^c	Brain-Stem Dysgenesis	MTS	Other ^d						
1:																			
4: c.613C→T	Homozygous	9	p.Arg205X	34	Moroccan	-	+	+	+	DWM	+	?	IUGR						
5: c.613C→T	Homozygous	9	p.Arg205X	18		-	+	?	-	OE	?	?							
2:																			
312: c.3175delA	Homozygous	28	p.Ile1059X	27	Tunisian	-	+	Focal	-	OM, CVA hydrocephaly	+	?	Microphthalmia, lung hypoplasia						
3:																			
0114: No DNA				33	Tunisian	+	+	+	-	?			ASD, VSD						
4467: No DNA				17		+	+	+	-	?									
1530: No DNA				19		+	+	+	-	DWM									
1189: No DNA				20		+	+	+	-	DWM, CCH, ARH	+	?							
2607: c.384_387delTAGA	Homozygous	6	p.Asp128GlufsX34	18		+	+	+	-	DWM	+	+							
3501: c.384_387delTAGA	Homozygous	6	p.Asp128GlufsX34	20		-	+	+	-	DWM	+	-							
4:																			
304: c.180+2 T→A	Father	3	Splice	19	Tunisian (father)	-	+	+	-	OM, CVH	+	+							
c.384_387delTAGA	Mother	6	p.Asp128GlufsX34																
303: c.180+2 T→A	Father	3	Splice	16	French (mother)	-	+	+	-	OM, CVH	+	+							
c.384_387delTAGA	Mother	6	p.Asp128GlufsX34																
5:																			
408: No DNA				29	French	-	+	-		OM, DWM, hydrocephaly, ARH, CVH, cystic V4	?	?	Situs inversus						

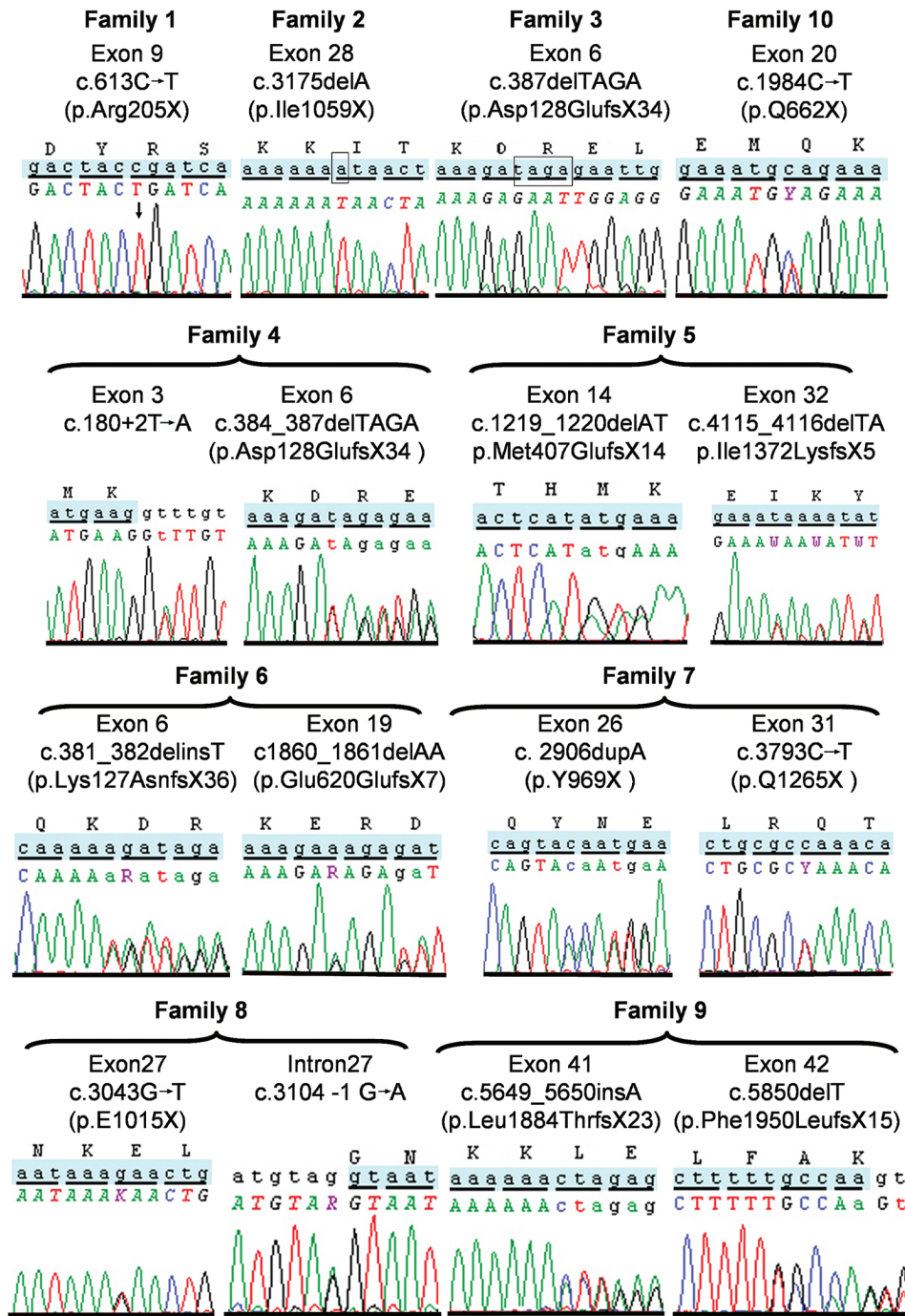


Figure 3. Sequence chromatographs of *CEP290* mutations identified in the present study. Mutation numbering is based on cDNA sequence, where +1 corresponds to the A of the ATG translation codon in the GenBank cDNA reference sequence NM_025114.3. The predicted effect of the mutation on the protein is also given with the amino acid number.

same intronic mutation located in intron 26 (c.2991+1655A→G) leading to an aberrant transcript and premature stop codon. Patients were either homozygous for this mutation and retained some normal transcript or were compound heterozygous for another *CEP290* mutation. The 299+1644A→G mutation is found exclusively in patients with LCA, although a recent study identified pa-

tients with LCA with two truncating *CEP290* mutations but not the intron 26 mutation.¹¹ No other genotype-phenotype correlations have been observed for *CEP290* mutations leading to JS, MKS, or LCA phenotypes. All *CEP290* mutations reported so far are truncating in all three phenotypes, except for two missense mutations reported in two patients with JS: p.W7C²⁰ and p.A1991G.²¹ *TMEM67*

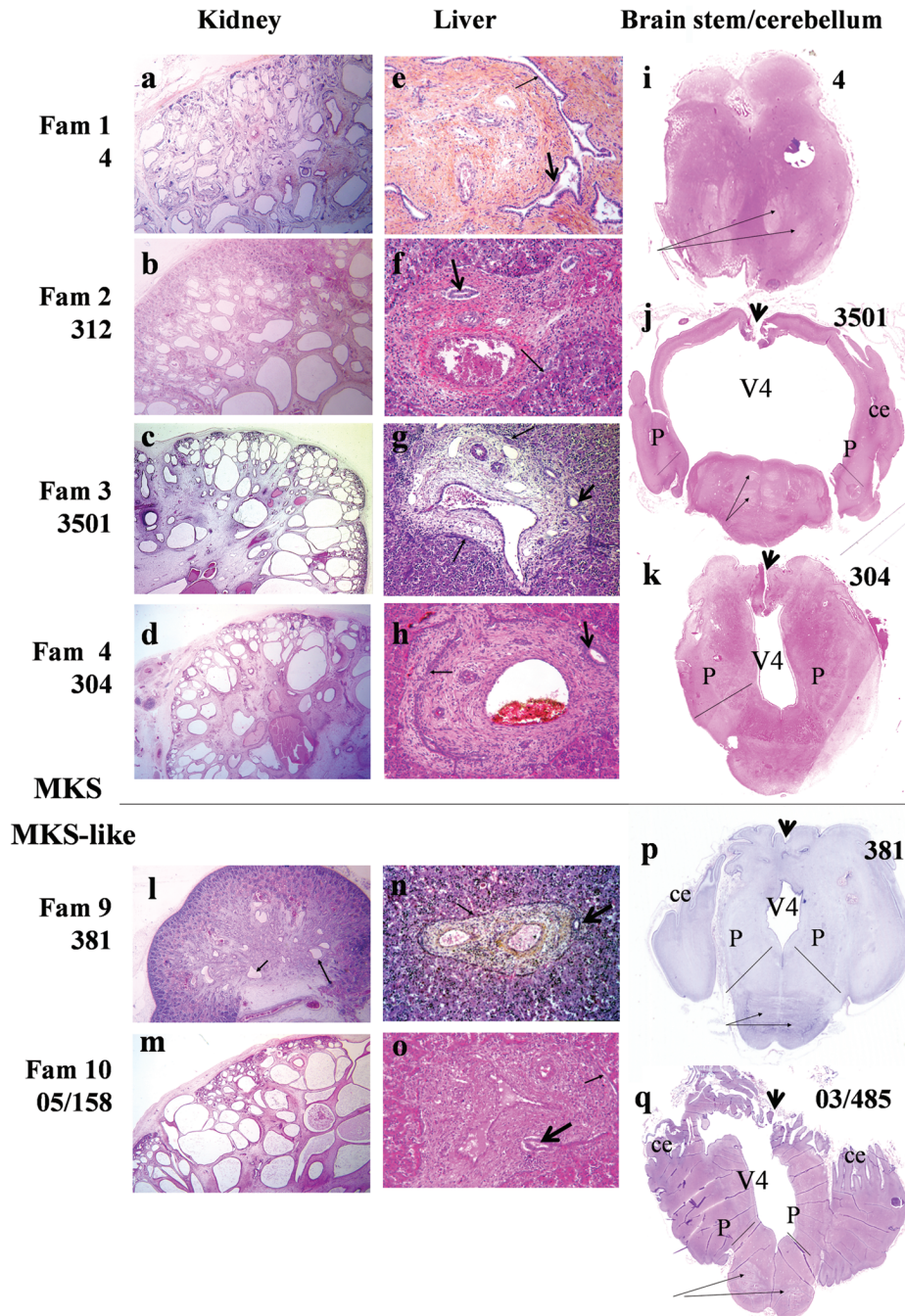


Figure 4. Pathological features of fetal cases with *CEP290* mutations. Histological sections (HES staining) of kidney (left), liver (middle), and brain stem/cerebellum (right) of MKS- and MKS-like-affected fetuses with *CEP290* mutations. In families 1–4 (a–d) and 10 (m), kidney histology shows major abnormalities characteristic of MKS: cysts in both kidney and medulla, growing from periphery to center. Small areas of conserved nephrogenesis are observed in the subcapsular zone. In family 9 (l), kidney histology shows conserved corticomedullary organization with several generations of mature glomeruli. Microcysts are found in the deep cortex, but tubular microcysts are observed mainly in medulla (black arrows). Liver histology shows a portal fibrosis with persistent ductal plate (arrows) and/or BDP/dilatation (arrowheads). Subject 4 (b) had the most-severe liver fibroadenomatosis, whereas the liver anomalies were moderate and focal in families 9 (n) and 10 (o). Brain-stem/cerebellum transverse sections are shown for five cases. i, Subject 4: section of the mesencephalon showing the chaotic organization of fibers and tracts (arrows) and atretic aqueduct of Sylvius. j, Subject 3501: section at the level of the pons showing severely dilated V4, enlarged cerebellar peduncle (P), chaotic organization of fibers and tracts (arrows), hypoplastic vermis (arrowhead), and cerebellar hemispheres (ce). k, Fetus 304. Note the inverted MTS with dysmorphic V4 flanked with enlarged and elongated cerebellar peduncles (P). For fetuses 381 (p) and 03/485 (q), the section at the level of the pons shows an inverted MTS with chaotic fibers and tracts (arrows), dysmorphic V4, severe hypoplasia of vermis (arrowhead), and well-developed cerebellar hemispheres. Fam = family.

mutations are either truncating or missense in both JS and MKS.¹⁹ Further functional analyses are needed to clarify whether the nature of the mutations is responsible for the variable clinical spectrum observed with *CEP290* or *TMEM67* mutations. However, the existence of both phenotypes in siblings—or the same mutation leading to different phenotypes—argues against this hypothesis for *CEP290*. In view of the oligogenic inheritance and epistatic mutations already reported for JS²¹ and BBS,^{24,25} mutations/polymorphisms in other ciliary protein-encoding genes is a tantalizing alternative hypothesis. In family 10, we identified only one *CEP290* nonsense mutation (p.Q662X) inherited from the father and two fetuses that were haploidentical at the locus; we may have failed to find the maternal *CEP290* molecular event. The other possibility, within the context of oligogenism, is that the recessive mutation is in another gene. However, we failed to find any mutations in the *MKS1*, *TMEM67*, or *BBS1–BBS10* genes in this family.

Along the same line, it is noteworthy that, in family 1, originating from Morocco (fig. 1c), two distinct ciliopathies segregated in the kindred—namely, autosomal recessive polycystic kidney disease (ARPKD) (in the first child and fetus 6) and JS/MKS (in fetuses 5 and 6). The diagnosis of ARPKD was confirmed through kidney and liver histology. The *CEP290* p.R205X mutation was found at the homozygous state only in siblings 5 and 6 with the MKS phenotype. The *PKHD1* locus showed homozygosity in subject 6 with ARPKD, compatible with a homozygous *PKHD1* mutation. Interestingly, homozygosity at the *PKHD1* locus was also observed in subject 4 with MKS, who had the most-severe kidney and liver phenotypes.

MKS is genetically and clinically heterogeneous. *MKS1* gene mutations were identified only in fetuses with the complete spectrum of MKS,¹ and, in a recent series, half of the fetuses had skeletal dysplasia with long-bone bowing or IUGR,⁵ a feature that was not observed in *TMEM67*-mutated fetuses and was present only in 1 of 21 siblings of our series with *CEP290* mutations. PD was much more frequent in *MKS1*-affected fetuses than in those with the *TMEM67* mutation and remains rare in *CEP290*-mutated fetuses (3 of 10 families; 8 of 20 fetuses). Since *MKS1* mutations were not identified in fetuses with either MKS-like or postnatal JS,¹⁹ one can hypothesize that MKS is at the very end of the spectrum of another human disorder. Hypomorphic *MKS1* mutations could cause another human ciliopathy in which, unlike JS, PD would be a frequent sign. In favor of this hypothesis, all *MKS1* mutations identified so far in MKS predict a truncated protein. The allelic nature of MKS and JS conditions may be extended to the *MKS2* locus, which has been mapped to chromosome 11q13⁴ and may therefore be allelic to *CORS2*, which has been mapped to 11p12–11q13.3.¹⁸ Indeed, whereas no organ involvement is described in patients with linkage to *JBTS1* on chromosome 9, a large variability is associated with *JBTS2*-linked patients, with multivisceral in-

volvement, including OE, PD, microphthalmia, and kidney involvement.²⁶

This study identifies a fourth locus for MKS (*MKS4*) and the *CEP290* gene on chromosome 12 as responsible for MKS. These data also further confirm the allelism between JS and MKS and extend the phenotypic spectrum of *CEP290* mutations already involved in JS and isolated LCA to a severe and lethal cystic kidney dysplasia with BDP of liver and neural-tube defects. Further studies will tell whether other genes might be responsible for both phenotypes and whether MKS might also represent the most severe, lethal end of the spectrum of other human ciliopathies.

Acknowledgments

We thank the patients and their families for participation. We thank Géraldine Goudefroye, for technical assistance, and the Société Française de Foetopathologie, for clinical data and material support. The genomewide scan with microsatellite markers was performed at Genoscope (by Prof. Jean Weissenbach). Support has been provided by National Institutes of Health grant R01 NS039818-09 (to M.V.). We thank Marcy Speer for collaboration on neural-tube defects projects. L.B. is supported by a postdoctoral fellowship from INSERM.

Web Resources

The URLs for data presented herein are as follows:

GenBank, <http://ncbi.nlm.nih.gov/Genbank/> (for cDNA translation codon [accession number NM_025114.3])
Online Mendelian Inheritance in Man (OMIM), <http://www.ncbi.nlm.nih.gov/Omim/> (for MKS, Meckel-like/Goldston syndrome, JS, LCA, and BBS)
UCSC Genome Browser, <http://genome.ucsc.edu/>

References

1. Kyttala M, Tallila J, Salonen R, Kopra O, Kohlschmidt N, Paavola-Sakki P, Peltonen L, Kestila M (2006) *MKS1*, encoding a component of the flagellar apparatus basal body proteome, is mutated in Meckel syndrome. *Nat Genet* 38:155–157
2. Smith UM, Consugar M, Tee LJ, McKee BM, Maina EN, Whelan S, Morgan NV, Goranson E, Gissen P, Lilliquist S, et al (2006) The transmembrane protein meckelin (*MKS3*) is mutated in Meckel-Gruber syndrome and the wpk rat. *Nat Genet* 38:191–196
3. Dawe HR, Smith UM, Cullinane AR, Gerrelli D, Cox P, Badano JL, Blair-Reid S, Sriram N, Katsanis N, Attie-Bitach T, et al (2007) The Meckel-Gruber syndrome proteins *MKS1* and meckelin interact and are required for primary cilium formation. *Hum Mol Genet* 16:173–186
4. Roume J, Genin E, Cormier-Daire V, Ma HW, Mehaye B, Attie T, Razavi-Encha F, Fallet-Bianco C, Buenerd A, Clerget-Darpoux F, et al (1998) A gene for Meckel syndrome maps to chromosome 11q13. *Am J Hum Genet* 63:1095–1101
5. Khaddour R, Smith U, Baala L, Martinovic J, Clavering D, Shaffiq R, Ozilou C, Cullinane A, Kyttälä M, Shalev S, et al (2007) Spectrum of *MKS1* and *MKS3* mutations in Meckel syndrome: a genotype-phenotype correlation. *Hum Mutat* 28:523–524

6. Abecasis GR, Cherny SS, Cookson WO, Cardon LR (2002) Merlin—rapid analysis of dense genetic maps using sparse gene flow trees. *Nat Genet* 30:97–101
7. Woods CG, Valente EM, Bond J, Roberts E (2004) A new method for autozygosity mapping using single nucleotide polymorphisms (SNPs) and EXCLUDEAR. *J Med Genet* 41: e101
8. Sayer JA, Otto EA, O'Toole JF, Nurnberg G, Kennedy MA, Becker C, Hennies HC, Helou J, Attanasio M, Fausett BV, et al (2006) The centrosomal protein nephrocystin-6 is mutated in Joubert syndrome and activates transcription factor ATF4. *Nat Genet* 38:674–681
9. Valente EM, Brancati F, Silhavy JL, Castori M, Marsh SE, Barrano G, Bertini E, Boltshauser E, Zaki MS, Abdel-Aleem A, et al (2006) *AH11* gene mutations cause specific forms of Joubert syndrome-related disorders. *Ann Neurol* 59:527–534
10. den Hollander AI, Koenekoop RK, Yzer S, Lopez I, Arends ML, Voesenek KE, Zonneveld MN, Strom TM, Meitinger T, Brunner HG, et al (2006) Mutations in the *CEP290* (*NPHP6*) gene are a frequent cause of Leber congenital amaurosis. *Am J Hum Genet* 79:556–561
11. Perrault I, Delphin N, Hanein S, Gerber S, Dufier JL, Roche O, Defoort-Dhellemmes S, Dollfus H, Fazzi E, Munnich A, et al (2007) Spectrum of *NPHP6/CEP290* mutations in Leber congenital amaurosis and delineation of the associated phenotype. *Hum Mutat* 28:416
12. Joubert M, Eisenring JJ, Andermann F (1968) Familial dysgenesis of the vermis: a syndrome of hyperventilation, abnormal eye movements and retardation. *Neurology* 18:302–303
13. Patel S, Barkovich AJ (2002) Analysis and classification of cerebellar malformations. *AJNR Am J Neuroradiol* 23:1074–1087
14. Ferland RJ, Eyaid W, Collura RV, Tully LD, Hill RS, Al-Nouri D, Al-Rumayyan A, Topcu M, Gascon G, Bodell A, et al (2004) Abnormal cerebellar development and axonal decussation due to mutations in *AH11* in Joubert syndrome. *Nat Genet* 36:1008–1013
15. Parisi MA, Bennett CL, Eckert ML, Dobyns WB, Gleeson JG, Shaw DW, McDonald R, Eddy A, Chance PF, Glass IA (2004) The *NPHP1* gene deletion associated with juvenile nephronophthisis is present in a subset of individuals with Joubert syndrome. *Am J Hum Genet* 75:82–91
16. Saar K, Al-Gazali L, Sztriha L, Rueschendorf F, Nur-E-Kamal M, Reis A, Bayoumi R (1999) Homozygosity mapping in families with Joubert syndrome identifies a locus on chromosome 9q34.3 and evidence for genetic heterogeneity. *Am J Hum Genet* 65:1666–1671
17. Valente EM, Salpietro DC, Brancati F, Bertini E, Galluccio T, Tortorella G, Briuglia S, Dallapiccola B (2003) Description, nomenclature, and mapping of a novel cerebello-renal syndrome with the molar tooth malformation. *Am J Hum Genet* 73:663–670
18. Keeler LC, Marsh SE, Leeflang EP, Woods CG, Sztriha L, Al-Gazali L, Gururaj A, Gleeson JG (2003) Linkage analysis in families with Joubert syndrome plus oculo-renal involvement identifies the *CORS2* locus on chromosome 11p12-q13.3. *Am J Hum Genet* 73:656–662
19. Baala L, Romano S, Khaddour R, Saunier S, Smith UM, Audolent S, Ozilou C, Faivre L, Laurent N, Foliguet B, et al (2007) The Meckel-Gruber syndrome gene, *MKS3*, is mutated in Joubert syndrome. *Am J Hum Genet* 80:186–194
20. Valente EM, Silhavy JL, Brancati F, Barrano G, Krishnaswami SR, Castori M, Lancaster MA, Boltshauser E, Boccone L, Al-Gazali L, et al (2006) Mutations in *CEP290*, which encodes a centrosomal protein, cause pleiotropic forms of Joubert syndrome. *Nat Genet* 38:623–625
21. Tory K, Lacoste T, Burglen L, Morinière V, Boddaert N, Macher M, Llanas B, Nivet H, Bensman A, Niaudet P, et al (2007) High *NPHP1* and *NPHP6* mutation rate in patients with Joubert syndrome and nephronophthisis: epistatic effect of *NPHP6* and *AH11* mutations in patients with *NPHP1* mutations. *J Am Soc Nephrol* 18:1566–1575
22. Ahdab-Barmada M, Claassen D (1990) A distinctive triad of malformations of the central nervous system in the Meckel-Gruber syndrome. *J Neuropathol Exp Neurol* 49:610–620
23. Karmous-Benaïly H, Martinovic J, Gubler M-C, Sirot Y, Clech L, Ozilou C, Augé J, Brahimi N, Etchevers H, Detrait E, et al (2005) Antenatal presentation of Bardet-Biedl syndrome may mimic Meckel syndrome. *Am J Hum Genet* 76:493–504
24. Katsanis N (2004) The oligogenic properties of Bardet-Biedl syndrome. *Hum Mol Genet Suppl* 13:R65–R71
25. Badano JL, Leitch CC, Ansley SJ, May-Simera H, Lawson S, Lewis RA, Beales PL, Dietz HC, Fisher S, Katsanis N (2006) Dissection of epistasis in oligogenic Bardet-Biedl syndrome. *Nature* 439:326–330
26. Valente EM, Marsh SE, Castori M, Dixon-Salazar T, Bertini E, Al-Gazali L, Messer J, Barbot C, Woods CG, Boltshauser E, et al (2005) Distinguishing the four genetic causes of Joubert syndrome-related disorders. *Ann Neurol* 57:513–519